Sivanesan *et al. J Nanobiotechnol (2015) 13:43*
DOI 10.1186/s12951-015-0102-8

JOURNAL OF NANOBIOTECHNOLOGY

RESEARCH Open Access

Reproducible and label-free biosensor for the selective extraction and rapid detection of proteins in biological fluids

Arumugam Sivanesan[1], Emad L Izake[1*], Roland Agoston[1], Godwin A Ayoko[1] and Martin Sillence[2]

Abstract

Erythropoietin (EPO), a glycoprotein hormone of ~34 kDa, is an important hematopoietic growth factor, mainly produced in the kidney and controls the number of red blood cells circulating in the blood stream. Sensitive and rapid recombinant human EPO (rHuEPO) detection tools that improve on the current laborious EPO detection techniques are in high demand for both clinical and sports industry. A sensitive aptamer-functionalized biosensor (aptasensor) has been developed by controlled growth of gold nanostructures (AuNS) over a gold substrate (pAu/AuNS). The aptasensor selectively binds to rHuEPO and, therefore, was used to extract and detect the drug from horse plasma by surface enhanced Raman spectroscopy (SERS). Due to the nanogap separation between the nanostructures, the high population and distribution of hot spots on the pAu/AuNS substrate surface, strong signal enhancement was acquired. By using wide area illumination (WAI) setting for the Raman detection, a low RSD of 4.92% over 150 SERS measurements was achieved. The significant reproducibility of the new biosensor addresses the serious problem of SERS signal inconsistency that hampers the use of the technique in the field. The WAI setting is compatible with handheld Raman devices. Therefore, the new aptasensor can be used for the selective extraction of rHuEPO from biological fluids and subsequently screened with handheld Raman spectrometer for SERS based in-field protein detection.

Keywords: Aptamer-functionalized biosensor (aptasensor), Nanosensor, Homogenous SERS, Wide area illumination, Erythropoietin (EPO), Horse plasma

Background

Erythropoietin (EPO), a glycoprotein hormone of ~ 34 kDa, is an important hematopoietic growth factor, mainly produced in the kidney and controls the number of red blood cells circulating in the blood stream [1]. After the establishment of human EPO gene sequence [2], recombinant human EPO (rHuEPO), a structural and bioactive analogue of human EPO, has been produced as a pharmaceutical to treat patients suffering from anaemia symptoms associated with various disorders such as cancer [3]. rHuEPO has also been used by athletes as a doping agent in endurance sports to enhance their performance [4]. This prompted World Anti-Doping Agency (WADA) to ban the use of the drug in sports activities [1]. In addition to its chief function in promoting erythropoiesis, it was recently indicated that EPO levels in cancer patients, especially when receiving chemotherapy, may significantly affect the growth and progression of malignant tumours [5, 6]. Thus, sensitive and rapid rHuEPO detection tools are in high demand for both clinical and sports industry [7].

In recent years, SERS has emerged as an ultra-sensitive analytical tool [8–10]. The two important features for real world applications of SERS are the homogeneity of the SERS substrate and selectivity towards target [11]. Vast numbers of SERS active surfaces comprising various roughened metallic surfaces and noble metal nanostructures have been produced. However, the majority of surfaces failed to produce a homogeneous SERS signal. Conversely, very few substrates which are promising to deliver homogeneous and reproducible signal are

*Correspondence: e.kiriakous@qut.edu.au
[1] Nanotechnology and Molecular Sciences Discipline, Faculty of Science and Engineering, Queensland University of Technology, 2 George St., Brisbane, QLD 4001, Australia
Full list of author information is available at the end of the article

expensive [12]. Therefore, there is a high demand for cheap, homogeneous and reproducible SERS substrates. In principle, the basic requirement for a homogeneous and sensitive SERS substrate is defect-free arrangement of metal nanoparticles or nanostructures within nanometer scale inter-particle distance [13].

Electrodeposition of metal nanostructures is one of the simple, cost effective and efficient approaches that realize the defect-free packing of nanostructures over a wide area [14]. To enhance the selectivity within SERS, recognition molecules that specifically bind to targets can be immobilized on the SERS substrate. However, the size and length of the recognition molecule should not be very large otherwise the SERS effect may completely diminish due to the long distance between the captured protein and the plasmonic surface. In other words, the binding receptor should not be far away from the surface as SERS signal exponentially decreases with respect to the increase in distance between the surface and analyte.

Antibodies are frequently used as recognition molecules for detecting proteins. However, antibodies usually have large size that constitutes a serious hurdle to the label-free SERS detection of proteins [7]. Aptamers are now widely emerging as better choice over antibodies [15]. Aptamers are of much smaller size than antibodies and also well-known for their high selectivity, binding affinity, easy and quick production, stability and cost-effectiveness [16]. Moreover, aptamers can bend and orient themselves close to the surface of the SERS substrate after binding with the target protein [17]. This orientation would lead to high intensity SERS signal due to short distance between the captured target and SERS surface. Thus, this article presents a homogeneous and sensitive aptamer-functionalized nanosensor for the rapid reproducible and label-free SERS detection of rHuEPO in biological fluids.

Methods

Nanostructured SERS substrate (pAu/AuNS) was prepared by potentiostatic deposition of AuNS over mirror polished Au surface [14] (see Additional file 1).

Results and discussion

Characterization of SERS substrate

We optimized gold chloride concentration, electrolyte, applied potential and time to have a closely packed single layer of AuNS within nanometer scale inter-particle distance. Figure 1 shows the SEM pictures of pAu/AuNS surface. The SEM image under wider magnification (Figure 1a) illustrates that the deposition of AuNS is virtually uniform over the entire surface. Even at a 100 micron field of view, the particle coverage was uniform and defect free (Additional file 1: Figure S1). Similar SEM images were obtained over the entire 8 mm diameter pAu/AuNS disc surface which clearly reveals that the electrodeposition method produced homogeneous AuNS over the entire surface. Although the sizes of AuNS ranged between 10 and 100 nm (Figure 1b), the uniform close packing of AuNS in single layer lead to homogeneous SERS signal for a focused micron-scale laser spot [11] (vide infra). Polished Au was chosen as the underlying support since it produces more AuNS particle initiation spots during electrodeposition in contrast to glassy carbon or indium tin oxide surfaces [14]. As a result, high density of small-sized and closely packed AuNS was produced and led to enormous SERS enhancement. Furthermore, a possible coupling between the propagating surface plasmon polariton (SPP) of the underlying polished Au surface and surface plasmon resonance (SPR) of the AuNS [14, 18] may lead to additional SERS enhancement.

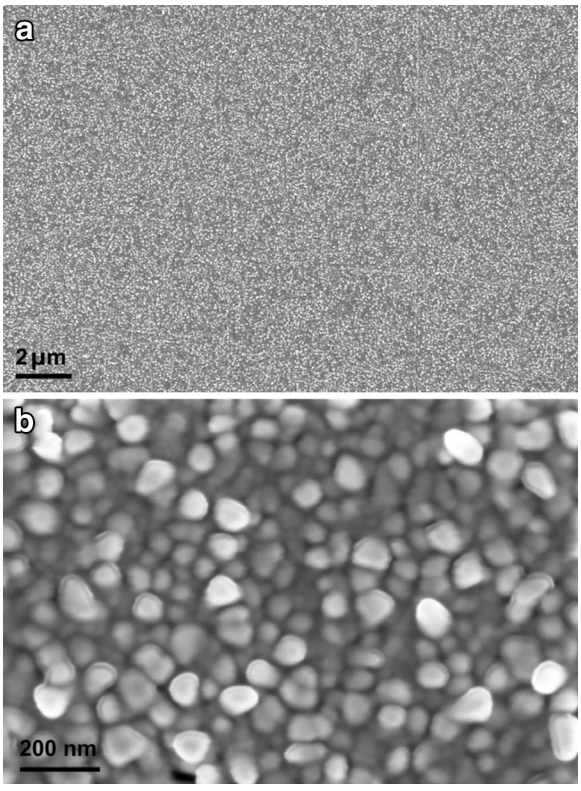

Figure 1 **a**–**b** SEM images of pAu/AuNS surface under different magnifications.

Reproducibility of SERS spectra

In order to test the homogeneity of the substrate and the reproducibility of the SERS signal from various locations on the sensor, we used 2-quinolinethiol (2-QT) as a probe molecule due to its large Raman scattering cross section. Additional file 1: Figure S2 depicts the SERS spectrum of the self-assembled monolayer of 2-QT over pAu/AuNS substrate. The intense band at 1,371 cm^{-1}, corresponding

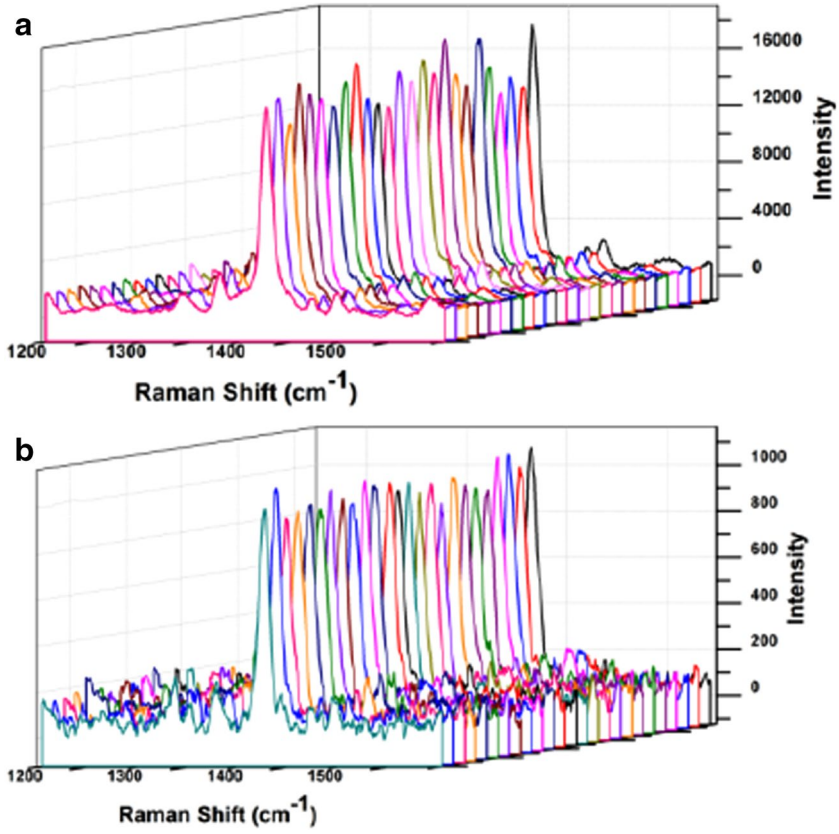

Figure 2 A series of SERS spectra of 2-QT randomly collected over the entire 8 mm diameter pAu/AuNS disc using **a** 50× objective with a laser focusing area of 0.32 μ^2 and **b** 5× objective with a laser focusing area of 12.56 μ^2.

to the aromatic ring stretching, was used to calculate the relative standard deviation (RSD) of the SERS signal intensity from various surface locations. For comparison purposes, we carried out the SERS measurements using used 5× (spot diameter = 3.99 μm; illuminated area = 12.56 μ^2 and working distance = 14 mm) and 50× (spot diameter = 0.64 μm; illuminated area = 0.32 μ^2 and working distance = 0.37 mm) objectives respectively. When the laser beam is focused using the 50× objective, the RSD of the SERS signal at 1,371 cm^{-1} (150 measurements from various surface spots, Figure 2a) was found to be 8.74%. However, the RSD reduces to 4.92% when using the 5× objective (Figure 2b). This decrease in RSD with increase in laser focusing area (5× objective has 39.25 times higher illumination area than 50× objective) is rational as the acquired SERS signal is highly averaged when increasing the focusing area.

Using a 5× objective to focus the laser beam onto the pAu/AuNS substrate creates a wide area illumination (WAI) setting which allows for an increased area of the pAu/AuNS surface to be probed when compared to the area probed by the 50× objective. The increase in the area probed by the laser excitation beam contributes to the reproducibility of the SERS signal [19, 20]. This is confirmed by the low RSD of 4.92% obtained when using the 5× objective. In other words, the WAI setting allows for averaging the SERS signal from a large surface area of the aptasensor and hence the low RSD of the SERS measurements. Also the homogeneity of the particle coverage and packing leads to homogeneous distribution of the hot spots to give reproducible SERS signals despite the polydispersity (10–100 nm) of AuNS.

Selective extraction and SERS investigation of rHuEPO in aqueous medium

The developed pAu/AuNS substrate was then functionalized with EPO-specific aptamer and the remaining bare sites on the surface backfilled with 6-mercapto hexanol (see Additional file 1) to create the aptasensor. The aptamers-functionalized nanosensor was then used for the selective capturing of rHuEPO from aqueous medium followed by the direct SERS detection of the captured protein. To acquire the native Raman fingerprint of rHu-EPO, we dropped 10 nM rHuEPO over a pristine pAu/AuNS surface and allowed it to dry in inert atmosphere. The subsequent SERS spectrum rHuEPO over non-functionalized surface is depicted in Figure 3aI.

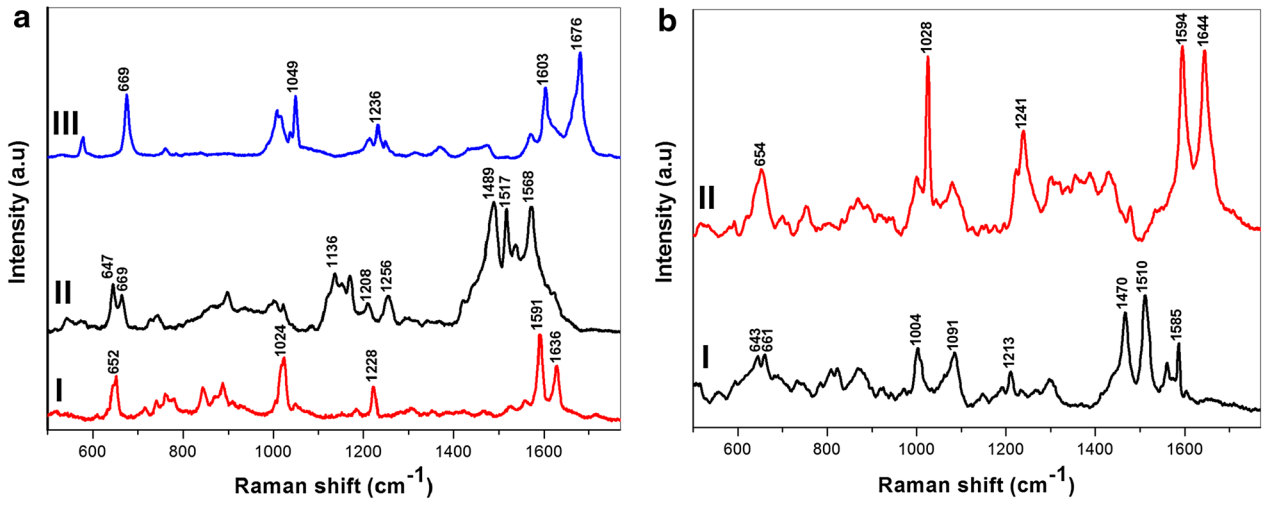

Figure 3 SERS spectra of **a** / pAu/AuNS/rHuEPO (drop dry), // pAu/AuNS/Apt (self-assembled monolayer) and /// pAu/AuNS/Apt/rHuEPO (selectively captured). **b** SERS spectra of pAu/AuNS/Apt incubated in / blank horse plasma and // rHuEPO spiked horse plasma. Each spectrum is the average of 10 spectra.

It is well known that the amide and aromatic (phenylalanine, tyrosine, tryptophan and histidine) vibrational bands dominates the Raman spectrum of proteins and polypeptides [21–27]. Similarly, the SERS spectrum of pAu/AuNS/rHuEPO (Figure 3aI) showed intense bands at 1,636 and 1,228 cm^{-1} corresponding to amide I and amide III vibrational modes, respectively [21–27]. The amide I at 1,636 cm^{-1} represent unique fingerprint of proteins as does not overlap with other vibrational modes from other functional groups. Therefore it can be used as a marker band for the identification of proteins without any external Raman labelling [28, 29].

The bands at 1,591 and 1,024 cm^{-1} correspond to the aromatic amino acid vibrational modes. Figure 3aII depicts the SERS spectrum of EPO aptamer on nanostructured surface. The SERS spectrum of an aptamer is usually dominated by adenine and guanine as the order of SERS cross–section is adenine > guanine > cytosine > thymine [30, 31]. Figure 3aII clearly indicated that the SERS spectrum of aptasensor is heavily dominated by the guanine vibrational modes at 647, 1,489 and 1,568 cm^{-1}. This is because the EPO aptamer has higher contribution from guanine nucleobase than adenine (13:5). Also, the C-S stretching mode for the thiolated aptamer is depicted at 669 cm^{-1}. Figure 3aIII shows the SERS spectrum of the apatsensor after capturing the rHuEPO protein (pAu/AuNS/Apt/rHuEPO) on its surface by the EPO aptamers. Scheme 1 depicts the graphical representation of rHuEPO captured aptasensor and subsequent SERS investigation. SERS The strong band at 1,676 cm^{-1} is attributed to the amide I vibrational mode [21–27]. The amide I band at 1,676 cm^{-1} is red shifted by 40 cm^{-1} when compared to

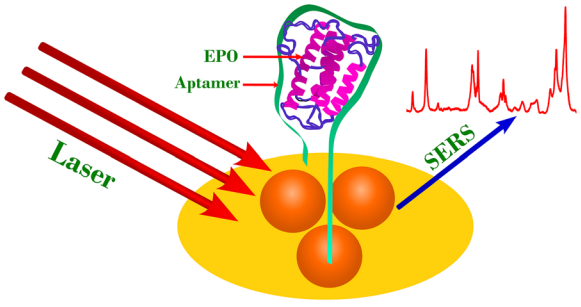

Scheme 1 Graphical representation of rHuEPO captured aptasensor and subsequent SERS investigation.

that of native rHuEPO at 1,636 cm^{-1} (Figure 3aI). Similarly, the vibrational modes of the aromatic amino acids at 1,603, 1,236 and 1,049 cm^{-1} are also red shifted. The shift in vibrational energy of the rHuEPO over the aptasensor surface is attributed to the aptamer conformational rearrangements upon binding rHuEPO to the aptamer fragment antigen binding (Fab) regions in the aqueous medium [7, 32].

In order to reveal the suitability of the present aptamer modified pAu/AuNS surface towards SERS quantification of rHuEPO, various concentrations of rHuEPO in aqueous medium were employed. To each concentration of rHuEPO, a freshly prepared pAu/AuNS/Apt surface was used to selectively capture rHuEPO onto the aptasensor surface and subsequently screened under the Raman microscope. Figure 4a shows the SERS spectra (amide 1 vibrational mode) of the pAu/AuNS/Apt/rHuEPO surface within a rHuEPO concentration range of 10 nM to

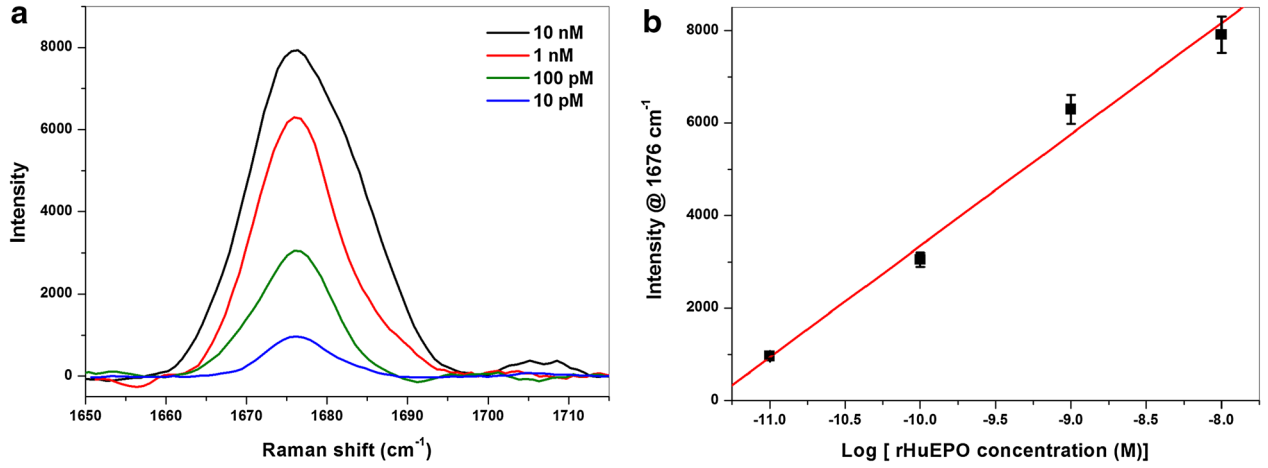

Figure 4 **a** SERS spectra of pAu/AuNS/Apt/rHuEPO with decreasing concentration of rHuEPO: 10 nM (*black*), 1 nM (*red*), 100 pM (*green*), and 10 pM (*blue*). **b** Plot demonstrating the linear relationship between log concentration of rHuEPO and SERS intensity at 1,676 cm^{-1}.

10 pM (the spectra were normalized and background subtracted). The band centered at 1,676 cm^{-1} corresponding to amide I vibrational mode of rHuEPO was used a reference band for rHuEPO quantification. The SERS signals were found to monotonically decrease with decreasing concentration (Figure 4a). A linear relationship was obtained between the SERS signal intensity at 1,676 cm^{-1} and the corresponding rHuEPO log concentration plot as depicted in Figure 4b. Similar linear relationship between log(concentration) and SERS intensity was formerly demonstrated in the literature [8, 33]. As indicated by Figure 4b, good correlation ($R^2 = 0.993$) was found over a wide concentration range of TNT (10^{-8} to 10^{-11} M).

Selective extraction and detection of rHuEPO in biological fluids

As a proof of concept for the SERS detection of EPO doping in biological fluids, we extended our methodology towards the label-free identification of rHuEPO in horse plasma. 1 nM rHuEPO was spiked into neat horse plasma and subsequently dropped over the pAu/AuNS/Apt. After 30 min, the substrate was washed with Millipore water to remove the biological matrix and dried in gentle flow of argon gas. A similar blank experiment was also carried out using un-spiked serum. Figure 3bI, II show the SERS spectra of blank and rHuEPO spiked (Figure 3bII), on aptasensor respectively. Figure 3bI shows strong correlation to Figure 3aII of the pAu/AuNS/Apt before interaction with EPO protein. The resemblance between Figure 3aII, bI indicates that the aptasensor when interacted with blank plasma matrix (no EPO spiked in matrix) did not bind with any of the non EPO proteins that exist in horse plasma. This result confirms the selectivity of the aptasensor towards its target protein over other proteins that may co-exist in a biological matrix. This Figure 3bII clearly depicted the amide I band at 1,644 cm^{-1} and aromatic amino acid vibrations at 1,594 and 1,028 cm^{-1}. A close comparison between Figure 3aI, bII confirms unambiguous resemblance between the spectrum of rHuEPO standard and that of the aptasensor after interacting with the plasma sample spiked with rHuEPO. The shifts in band positions between Figure 3aIII, bII may attributed in part to the higher dielectric constant and solvent polarity of aqueous matrix in comparison to those of the protein rich plasma matrix [34]. In Figure 3aIII, the higher dielectric constant and polarity of the aqueous matrix may have caused the red shift of the amid I band to the higher wave number of 1,676 cm^{-1} from its position at 1,636 cm^{-1} in Figure 3aI, bII. Therefore, we have successfully demonstrated the selective extraction and SERS identification of rHuEPO in horse plasma. This outcome clearly indicates the significance of using aptamers-functionalized homogeneous SERS substrate for facile and rapid screening of proteins in biological fluids. The full potential of the aptasensor is realized when it is combined with handheld Raman device for the in-field detection of rHuEPO from biological matrices.

Conclusion

We demonstrated a sensitive and homogenous aptasensor for the reproducible detection of EPO in biological fluids. Due to the close packing and homogenous distribution of the nanoparticles coverage over the surface, strong and reproducible signal enhancement is acquired

especially under WAI conditions where the RSD of the SERS measurements can be as low as 4.92%. By adapting to wide area, handheld Raman devices can used in combination with the new aptasensor for the label-free in-field screening of rHuEPO in horse plasma.

Additional file

Additional file 1. Experimental producers to fabricate reproducible aptamer-functionalized SERS substrate as well as the detection of EPO in horse plasma are given in this document.

Abbreviations

EPO: erythropoietin; rHuEPO: recombinant human EPO; SERS: surface enhanced Raman spectroscopy; AuNS: gold nanostructures; pAu/AuNS: gold nanostructures over a gold substrate; aptasensor: aptamer-functionalized biosensor; WAI: wide area illumination; 2-QT: 2-quinolinethiol.

Authors' contributions

AS carried out the manufacture of the new substrate, Raman measurements and drafted the manuscript. ELI conceived of the study, and participated in its design and coordination and helped to draft the manuscript. RA contributed to the experimental design and measurements and to the preparation of the draft. GAA participated in the design of the study and contributed to the preparation of the draft. MS participated in the design of the study and contributed to the preparation of the draft. All authors read and approved the final manuscript.

Author details

[1] Nanotechnology and Molecular Sciences Discipline, Faculty of Science and Engineering, Queensland University of Technology, 2 George St., Brisbane, QLD 4001, Australia. [2] Discipline of Biosciences, Faculty of Science and Engineering, Queensland University of Technology, 2 George St., Brisbane, QLD 4001, Australia.

Acknowledgements

The authors are grateful for the funding support from the Partnership for Clean Competition (PCC) research scheme (USA), Grant Number (RM2013000476).

Compliance with ethical guidelines

Competing interests

The authors declare that they have no competing interests.

Received: 26 February 2015 Accepted: 5 June 2015
Published online: 24 June 2015

References

1. Fisher JW (2003) Erythropoietin: physiology and pharmacology update. Exp Biol Med (Maywood) 228(1):1–14
2. Jacobs K, Shoemaker C, Rudersdorf R, Neill SD, Kaufman RJ, Mufson A et al (1985) Isolation and characterization of genomic and cDNA clones of human erythropoietin. Nature 313(6005):806–810
3. Henke M, Laszig R, Rube C, Schafer U, Haase KD, Schilcher B et al (2003) Erythropoietin to treat head and neck cancer patients with anaemia undergoing radiotherapy: randomised, double-blind, placebo-controlled trial. Lancet 362(9392):1255–1260. doi:10.1016/S0140-6736(03)14567-9
4. Parisotto R, Wu M, Ashenden MJ, Emslie KR, Gore CJ, Howe C et al (2001) Detection of recombinant human erythropoietin abuse in athletes utilizing markers of altered erythropoiesis. Haematologica 86(2):128–137
5. Yasuda Y, Fujita Y, Matsuo T, Koinuma S, Hara S, Tazaki A et al (2003) Erythropoietin regulates tumour growth of human malignancies. Carcinogenesis 24(6):1021–1029. doi:10.1093/carcin/bgg060
6. Schache AG, Liloglou T, Risk JM, Filia A, Jones TM, Sheard J et al (2011) Evaluation of human papilloma virus diagnostic testing in oropharyngeal squamous cell carcinoma: sensitivity, specificity, and prognostic discrimination. Clin Cancer Res Off J Am Assoc Cancer Res 17(19):6262–6271. doi:10.1158/1078-0432.CCR-11-0388
7. Hughes J, Izake EL, Lott WB, Ayoko GA, Sillence M (2014) Ultra sensitive label free surface enhanced Raman spectroscopy method for the detection of biomolecules. Talanta 130:20–25. doi:10.1016/j.talanta.2014.06.012
8. Jamil AKM, Izake EL, Sivanesan A, Agoston R, Ayoko GA (2015) A homogeneous surface-enhanced Raman scattering platform for ultra-trace detection of trinitrotoluene in the environment. Anal Methods 7(9):3863–3868. doi:10.1039/c5ay00739a
9. Sivanesan A, Witkowska E, Adamkiewicz W, Dziewit L, Kaminska A, Waluk J (2014) Nanostructured silver-gold bimetallic SERS substrates for selective identification of bacteria in human blood. Analyst 139(5):1037–1043. doi:10.1039/c3an01924a
10. Sivanesan A, Kozuch J, Ly HK, Kalaivani G, Fischer A, Weidinger IM (2012) Tailored silica coated Ag nanoparticles for non-invasive surface enhanced Raman spectroscopy of biomolecular targets. Rsc Adv 2(3):805–808. doi:10.1039/C1ra00781e
11. Ko H, Singamaneni S, Tsukruk VV (2008) Nanostructured surfaces and assemblies as SERS media. Small 4(10):1576–1599. doi:10.1002/smll.200800337
12. Kaminska A, Dziecielewski I, Weyher JL, Waluk J, Gawinkowski S, Sashuk V et al (2011) Highly reproducible, stable and multiply regenerated surface-enhanced Raman scattering substrate for biomedical applications. J Mater Chem 21(24):8662–8669. doi:10.1039/C0jm03336g
13. Natelson D, Li Y, Herzog JB (2013) Nanogap structures: combining enhanced Raman spectroscopy and electronic transport. Phys Chem Chem Phys 15(15):5262–5275. doi:10.1039/c3cp44142c
14. Sivanesan A, Adamkiewicz W, Kalaivani G, Kaminska A, Waluk J, Holyst R et al (2015) Towards improved precision in the quantification of surface-enhanced Raman scattering (SERS) enhancement factors: a renewed approach. Analyst 140(2):489–496. doi:10.1039/c4an01778a
15. Mascini M, Palchetti I, Tombelli S (2012) Nucleic acid and peptide aptamers: fundamentals and bioanalytical aspects. Angew Chem 51(6):1316–1332. doi:10.1002/anie.201006630
16. Lim YC, Kouzani AZ, Duan W (2010) Aptasensors: a review. J Biomed Nanotechnol 6(2):93–105
17. Feng L, Sivanesan A, Lyu Z, Offenhausser A, Mayer D (2015) Electrochemical current rectification-a novel signal amplification strategy for highly sensitive and selective aptamer-based biosensor. Biosens Bioelectron 66:62–68. doi:10.1016/j.bios.2014.10.057
18. Félidj N, Aubard J, Lévi G, Krenn JR, Schider G, Leitner A et al (2002) Enhanced substrate-induced coupling in two-dimensional gold nanoparticle arrays. Phys Rev B 66(24):245407
19. Shin K, Chung H (2013) Wide area coverage Raman spectroscopy for reliable quantitative analysis and its applications. Analyst 138(12):3335–3346. doi:10.1039/c3an36843b
20. Shin K, Ryu K, Lee H, Kim K, Chung H, Sohn D (2013) Au nanoparticle-encapsulated hydrogel substrates for robust and reproducible SERS measurement. Analyst 138(3):932–938. doi:10.1039/c2an35862j
21. Keyes TE, Leane D, Forster RJ, Moran N, Kenny D (eds) (2005) New insights into the molecular mechanisms of thrombosis from high resolution surface enhanced Raman microscopy. In: Proceedings of SPIE—the international society for optical engineering, 2005
22. Kurouski D, Postiglione T, Deckert-Gaudig T, Deckert V, Lednev IK (2013) Amide I vibrational mode suppression in surface (SERS) and tip (TERS) enhanced Raman spectra of protein specimens. Analyst 138(6):1665–1673. doi:10.1039/c2an36478f
23. Podstawka E, Ozaki Y, Proniewicz LM (2004) Adsorption of S–S containing proteins on a colloidal silver surface studied by surface-enhanced Raman spectroscopy. Appl Spectrosc 58(10):1147–1156. doi:10.1366/0003702042336073
24. Kumar GV, Selvi R, Kishore AH, Kundu TK, Narayana C (2008) Surface-enhanced Raman spectroscopic studies of coactivator-associated arginine methyltransferase 1. J Phys Chem B 112(21):6703–6707. doi:10.1021/jp711594z
25. Kundu PP, Bhowmick T, Swapna G, Kumar GVP, Nagaraja V, Narayana C (2014) Allosteric transition induced by Mg2+ ion in a transactivator monitored by SERS. J Phys Chem B 118(20):5322–5330. doi:10.1021/Jp5000733

26. Negri P, Chen G, Kage A, Nitsche A, Naumann D, Xu B et al (2012) Direct optical detection of viral nucleoprotein binding to an anti-influenza aptamer. Anal Chem 84(13):5501–5508. doi:10.1021/ac202427e
27. Blum C, Schmid T, Opilik L, Metanis N, Weidmann S, Zenobi R (2012) Missing amide I mode in gap-mode tip-enhanced raman spectra of proteins. J Phys Chem C 116(43):23061–23066. doi:10.1021/Jp306831p
28. Kahramana M, Wachsmann-Hogiu S (2015) Label-free and direct protein detection on 3D plasmonic nanovoid structures using surface-enhanced Raman scattering. Anal Chim Acta 856:74–81. doi:10.1016/j.aca.2014.11.019
29. Sane SU, Cramer SM, Przybycien TM (1999) A holistic approach to protein secondary structure characterization using amide I band Raman spectroscopy. Anal Biochem 269(2):255–272. doi:10.1006/abio.1999.4034
30. Barhoumi A, Zhang D, Tam F, Halas NJ (2008) Surface-enhanced Raman spectroscopy of DNA. J Am Chem Soc 130(16):5523–5529. doi:10.1021/ja800023j
31. Lu YL, Huang Q, Meng GW, Wu LJ, Zhang JJ (2014) Label-free selective SERS detection of PCB-77 based on DNA aptamer modified SiO2@Au core/shell nanoparticles. Analyst 139(12):3083–3087. doi:10.1039/C4an00197d
32. Mantelingu K, Kishore AH, Balasubramanyam K, Kumar GV, Altaf M, Swamy SN et al (2007) Activation of p300 histone acetyltransferase by small molecules altering enzyme structure: probed by surface-enhanced Raman spectroscopy. J Phys Chem B 111(17):4527–4534. doi:10.1021/jp067655s
33. Jamil AK, Izake EL, Sivanesan A, Fredericks PM (2015) Rapid detection of TNT in aqueous media by selective label free surface enhanced Raman spectroscopy. Talanta 134:732–738. doi:10.1016/j.talanta.2014.12.022
34. Sen KK, Basu SK, Dutta SK (2009) Binding studies of lamotrigine with sera of different animal species. Trop J Pharm Res 8(5):409–415